Torkan, Masoud; Hosseini Khorasgani , AMIR ; Uotinen, Lauri; Baghbanan, Alireza; Rinne, Mikael

Effect of anisotropy of fracture surface on fluid flow

Published in:
IOP Conference Series: Earth and Environmental Science

DOI:
10.1088/1755-1315/1124/1/012036

Published: 10/01/2023

Document Version
Publisher's PDF, also known as Version of record

Effect of anisotropy of fracture surface on fluid flow

IOP Conf. Series: Earth and Environmental Science 1124 (2023) 012036 doi:10.1088/1755-1315/1124/1/012036

Effect of anisotropy of fracture surface on fluid flow

Masoud Torkan[1*], Amir Hosseini Khorasgani[2], Lauri Uotinen[1], Alireza Bagbanan[2], Mikael Rinne[1]

[1] Department of Civil Engineering, School of Engineering, Aalto University, Finland
[2] Department of Mining Engineering, Isfahan University of Technology, Iran

masoud.torkan@aalto.fi

Abstract. Characterization of fluid flow through rough fractures is an important issue in designing underground excavations, such as nuclear repositories or geothermal applications. Fluid flow could be influenced by several parameters such as contact areas, aperture, hydraulic and mechanical conditions. Contact area and aperture could be two crucial geometrical factors which control hydraulic and mechanical behaviors of fractures. These factors are rarely isotropic, and anisotropy is observed in different directions. In this research, photogrammetry, as a high precision method, was used to analyze morphology of a tensile fracture induced in granite. Experimental and numerical stress-flow tests on rock fracture were conducted in two different directions with diverse normal stresses and water pressures. Analyzing the regenerated 3D model of the fracture and hydromechanical tests predicts the anisotropy in flow rates in different directions. Numerical and experimental results are well fitted particularly in low-stress conditions. The obtained results show that anisotropy affects permeability since outlet flow rates in the different directions with the same initial water pressures differ by 7 % in experiments and 4% in numerical modeling.

1. Introduction

Safe design of rock infrastructures depends on several factors, including mechanical and hydraulic properties of the rock mass. Among those affecting factors, hydraulic properties have a significant impact on instability and damage to these structures. Fluid flows cause several issues such as distributing stress states, transferring fluids containing hazardous substances, and instability. These cases can highlight the importance of studying groundwater and hydraulic properties at different stages of safety, initiation, and implementation in rock structures and different engineering projects such as underground excavations, slope designs, dam constructions, drilling, oil and gas recovery and extraction, geothermal reservoirs, and nuclear waste disposals [1].

Well-known models for groundwater analysis are not reliable in many cases. This is because they do not take into account the anisotropy and heterogeneity of rock mass due to lack of sufficient data, cost, and difficulty of measurement [2]. Several factors affect the flow regime in a single fracture, including the morphology of the fracture surface (for instance, roughness, anisotropy, aperture, and contact areas), scale effects, and effect of normal and shear stress [3].

Real surfaces of a fracture can be reconstructed and analyzed using different methods. Nondestructive techniques are a powerful tool for regenerating 3D fracture surfaces, such as laser scanning, injection, and photogrammetry. Photogrammetry can be used to reconstruct a 3D model by 2D images of an object. Nowadays, digital cameras and smartphones are used in the photogrammetric

method to regenerate 3D surfaces of a fracture, as a cheap, efficient, and accessible high-resolution method [4]. A fracture surface is usually naturally anisotropic because the distribution of asperities and their height at the fracture surfaces are nonidentical. The physical aperture and well-matedness of a fracture are able to determine the flow paths. In well-mated fractures, the amount of contact areas is almost higher. This could reduce flow paths through a fracture. Presence and shape of contact areas influence the degree of anisotropy of rock fractures. This could change hydraulic behavior in different directions [5].

In this regard, Auradou et al. [6] showed the anisotropy of the flow by laboratory studies using dyed fluid in a fracture with one transparent side to observe flow pathways through parallel and perpendicular shear directions. Based on a model of natural fractures, Gentier et al. [7] showed that permeability is clearly dependent on the direction of shear test. Méheust and Schmittbuhl [8] measured anisotropy by considering the direction of the pressure gradient and the geometric heterogeneity of the joint. Koyama et al. [1] performed numerical studies on the effect of anisotropy on flow at different scales, which shows during the direct shear test, the aperture was not identical, which causes anisotropy in the flow. Marchand et al. [9] demonstrated that flow anisotropy is dependent on changes in fracture aperture. Deng et al. [10] showed that anisotropy in hydraulic behavior depends on the anisotropy of the fracture geometry.

The aim of this study is to find the effect of anisotropy of a 25 × 25 cm rough fracture on the fluid flow in two perpendicular directions. The surfaces of the rock fracture were reconstructed by photogrammetry. Hydromechanical experiments were performed in perpendicular directions to evaluate the effect of anisotropy on fluid behavior at different water pressures and normal stresses. The fracture was modeled with numerical code and validated with laboratory data. Finally, the effect of anisotropy and its morphological effect with respect to numerical modeling are discussed.

2. Methodology

2.1. Photogrammetry procedure

The sample used in this study is a pair granite set of 250 mm × 250 mm × 100 mm slabs with an artificially induced tensile fracture (Figure 1a). The fracture surface looked very homogeneous with a visual inspection. A three-phase photogrammetric method was adopted to reconstruct a 3D model of a rough fracture. Sixteen circular markers were glued to the sample, and the distances among them were measured with a caliper with a resolution of 0.1 mm. The whole sample was photographed when the two halves were tightened together. Each half of the sample was scanned separately using a Canon 5DS R DSLR, Canon 35 mm f/1.4L II USM objective, and a rotary table. The scanning process was performed at the camera's 30° and 60° dip angles. Forty photos were captured in each dip angle (Figures 1b and 1c). The method's accuracy was improved by taking photos in 80° dip angle based on a 4×4 grid consisting of square cells, each with 5 cm side length. This resulted in taking 25 photos for each surface. The entire 3D exterior of the sample was reconstructed in RealityCapture 1.2 (Figure 1d). The obtained 3D model was scaled by the distances measured between circular markers with the caliper. The markers' coordinates were extracted from the georeferenced sample. Each half was regenerated and scaled with the markers' coordinates (Figure 1e). Finally, the physical aperture of the fracture was calculated with the Cloud-to-Cloud distance in CloudCompare software (Figure 1f).

2.2. Water flow test

Water flow tests were conducted using an experimental circuit illustrated in Figure 2. The circuit includes a hydraulic jack unit to apply normal stresses on the sample, a data logger to record data. A water tank, compressed air, and an adjustable air regulator apply constant water pressures to one side of the fracture. In order to measure the inlet water pressure, a pressure transducer was installed on the water inlet. A plate was used to equalize normal pressures on the top surface of the sample. The applied normal stresses were 0, 0.1, 0.3 and 0.5 MPa. The discharge water was weighed by a digital balance with a resolution of 0.01 g. Ten water pressures were chosen to perform water flow tests ranging from 5 kPa

to 50 kPa with 5 kPa intervals. The hydromechanical tests were done in the Department of Civil Engineering at Aalto University. The temperature was 25° C, and the density and dynamic viscosity of water are $\rho = 0.997\times10^{3}$ kg/m^{3} and $\mu=0.89\times10^{-3}$ Pa.s, respectively. A self-designed frame was built to seal the lateral sides of the sample (Figure 3). Pathways of inlets and outlets in preferred directions can control with this frame by valves. The rubber was glued to the internal faces of the frame to stop leakage of the water. Figure 4 shows the real sample, the frame, and the positions of LVDTs. Figure 5 illustrates the hydraulic boundary conditions used to analyze the fracture's anisotropy (First direction X (1 through 3) and Second direction Y (4 through 2)).

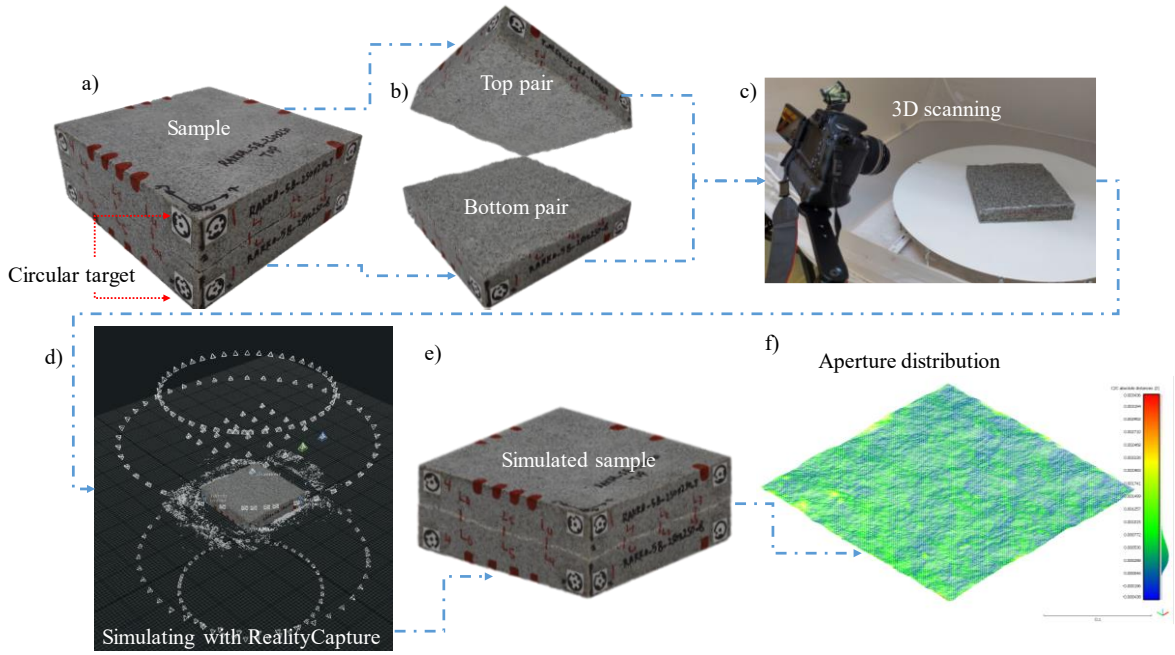

Figure 1. Photogrammetry and measurement procedures of fracture morphologies.

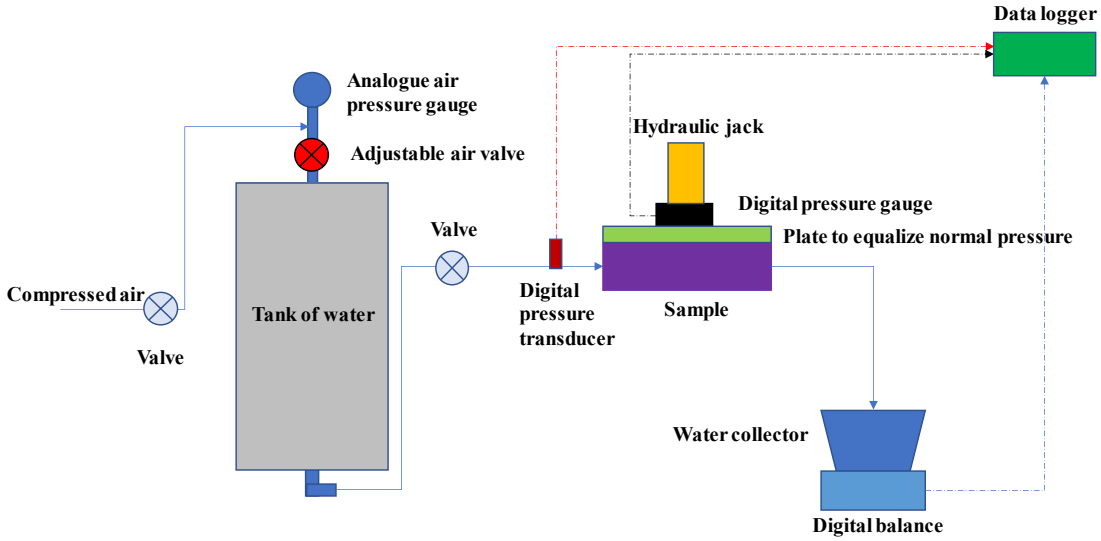

Figure 2. Schematic of the hydraulic test.

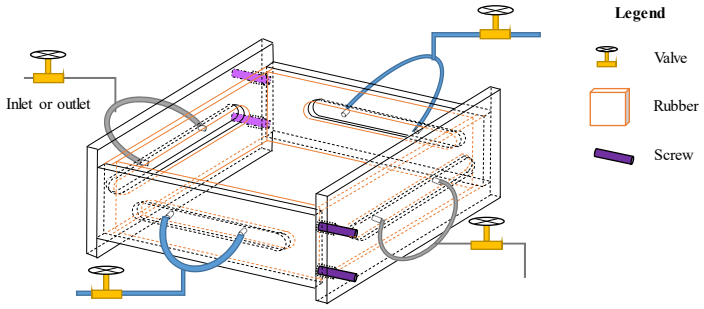

Figure 3. Diagram of the self-designed frame to test the water flow.

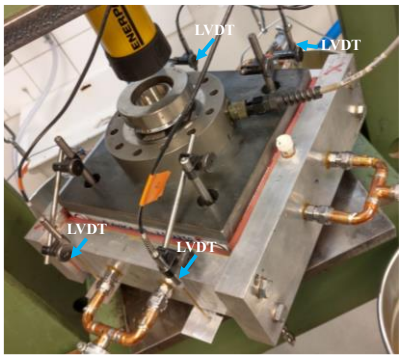

Figure 4. Locations of LVDTs.

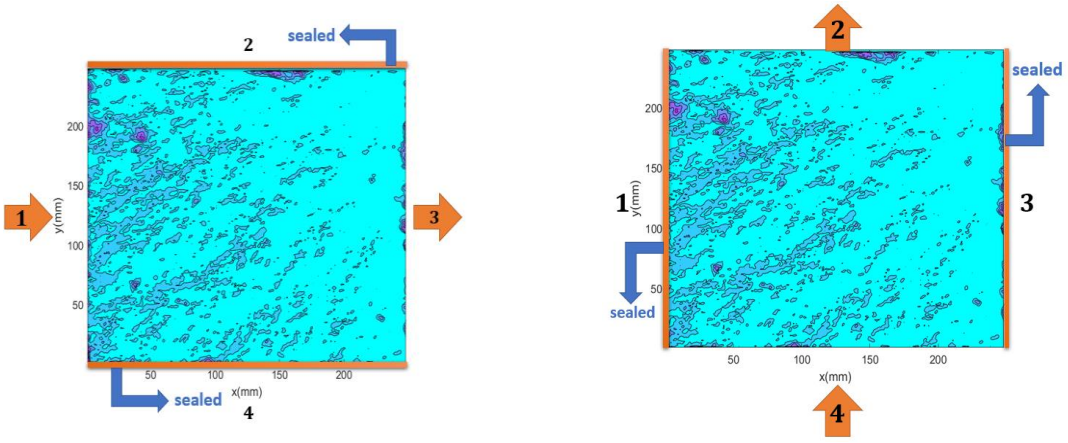

(a) (b)

Figure 5. Schemes of hydraulic boundary conditions.

2.3. Background theory

In order to characterize the flow through a rough fracture, the Forchheimer equation [11] is expressed as Equations (1), (2), (3):

$$-\nabla P = aQ + bQ^2 \tag{1}$$

$$a = \frac{12\mu}{we_h^3} \tag{2}$$

$$b = \frac{\beta\rho}{w^2 e_h^2} \tag{3}$$

Where ∇P signifies the hydraulic gradient (Pa/m), a (kg/m^{5}s) and b (kg/m^8) are viscous and inertial effects, respectively, Q denotes flowrate (m^3/s), w represents the width of the fracture (m), e_h is the hydraulic fracture (m), μ represents the dynamic viscosity of water (Pa.s), L is the length of the fracture (m) and β characterizes nonlinear coefficient, and ρ denotes the fluid density (kg/m^3).

In this study, numerical modeling using the Navier-Stokes equation for fluid as incompressible and single Newtonian fluid flow is facilitated as follows (Equations 4 to 7):

$$\frac{\partial u}{\partial t} + \nabla(u)u = F - \frac{1}{\rho}\nabla p + \frac{\mu}{\rho}\nabla^2 u \tag{4}$$

Where u is the velocity vector (m/s), t is the time (s), F is the physical force vector per mass unit (m/s^2), and p is the pressure (Pa). Due to the complexity and difficulty in solving Equation (4), the

simplified Equation (5) based on the developed Poiseuille current has been used alongside the Reynolds equation (Equations 6 and 7).

$$Q = -\frac{e^3}{12\mu}\nabla p \tag{5}$$

$$\nabla.(e^3\nabla p) = 0 \tag{6}$$

$$\frac{\partial}{\partial x}.(e^3(x,y)\frac{\partial p}{\partial x}) + \frac{\partial}{\partial y}.(e^3(x,y)\frac{\partial p}{\partial y}) = 0 \tag{7}$$

In this formula, e is aperture (m). The ratio ($b^3/12\mu$) is generally called fracture transmissivity. Since the transferability is proportional to the power of a third of aperture, this relationship is called the cube law.

2.4. Numerical modeling setup

Based on 4 to 7 equations, numerical code has been developed in MATLAB software, which in this code has been specified in order to determine the scope of software analysis, boundary conditions, and boundary range. Lateral fracture boundaries were defined as impermeable boundaries. Constant water pressure was applied along the inlet, and zero pressure was applied along with the outlet. The input information was then loaded based on the photogrammetry results and the water flow tests. These include the coordinates of the points and local apertures, the fluid properties, and the pressure gradient in each step. Output flow was calculated at each output node. In the geometry of the model, mesh size of 1 mm by 1 mm is considered, and the square model is 250 mm long. The numerical code was validated based on the experimental test when the normal stress was zero.

3. Results and discussion

The initial physical aperture, obtained by photogrammetry, was 0.3309 mm. After applying normal stresses 0.1, 0.3 and 0.5 MPa, the LVDTs' movements were averaged and physical apertures were calculated based on for each stage. The physical apertures 0.3218, 0.3005 and 0.2833, respectively. Increasing normal stress leads to enlarging contact areas. The morphology of the fracture is shown in Figures 6a and 6b under two different normal stresses, 0 MPa and 0.5 MPa, respectively.

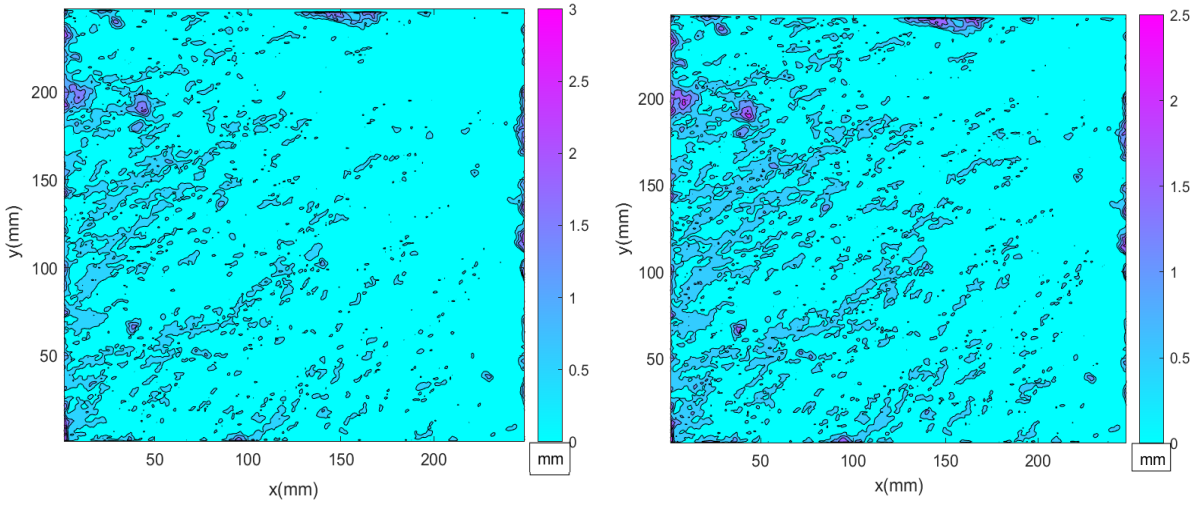

Figure 6. Fracture surface under two different normal stresses (a) 0 MPa and (b) 0.5 MPa.

The data obtained from experimental tests and numerical modeling are depicted in Figure 7. Forty water flow tests were performed in each direction (Figure 4). As it can be seen in Figure 7, tests' data are nonlinear, and it could be described by the Forchheimer equation. The accuracy of numerical modeling is almost 75%, according to flowrates.

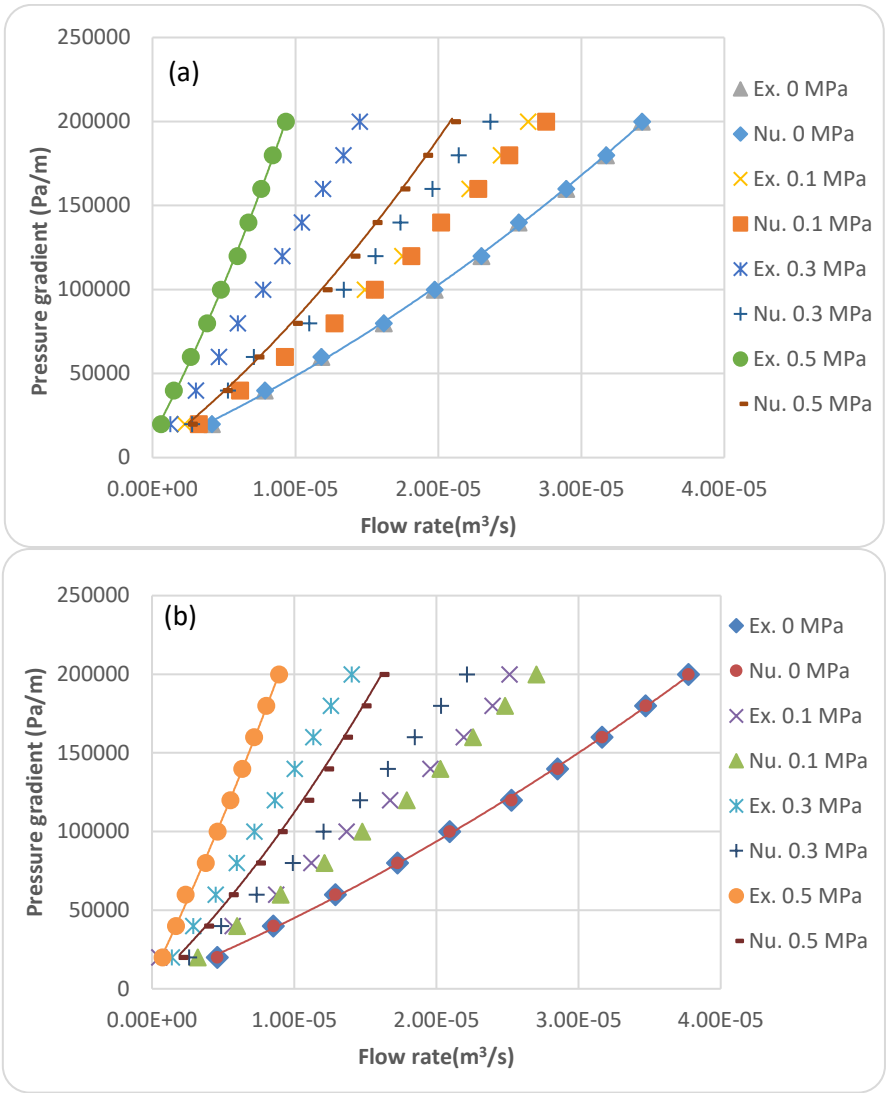

Figure 7. Experimental and numerical data analyzed with polynomial regression analysis of measured pressure gradient as a function of flow rate using the Forchheimer equation for the fracture under different normal stresses (a) through direction X (1 to 3) and (b) direction Y (4 to 2).

The difference between experimental flow rates in two different directions was 7% for all combinations. This difference could show the anisotropy of the fracture surface. The flow rate through direction Y is more considerable than direction X. Figure 8 illustrates the hydraulic apertures calculated by the Forchheimer equation for experimental and numerical tests through different directions. The numerical hydraulic apertures showed almost 88% agreement with the experimental results. Anisotropy is obvious by numerical modeling. The variation of the numerical hydraulic apertures between perpendicular directions was 4%.

Figure 9 shows simulations of the fracture surface for four different conditions. In Figures 9(a and b), flow was simulated through direction X with two different water pressures (5 and 50 kPa) and identical normal stress (0 MPa). New and robust streamlines could be observed by increasing the water pressure. Figures 9 (c and d) demonstrate streamlines through the direction Y after applying normal stress 0.5 MPa. The water pressures were 5 and 50 kPa. Notably, flow channels and streamline are totally different in two different directions. This is good evidence of an anisotropic surface because there are more void spaces and channels through direction Y compared with direction X.

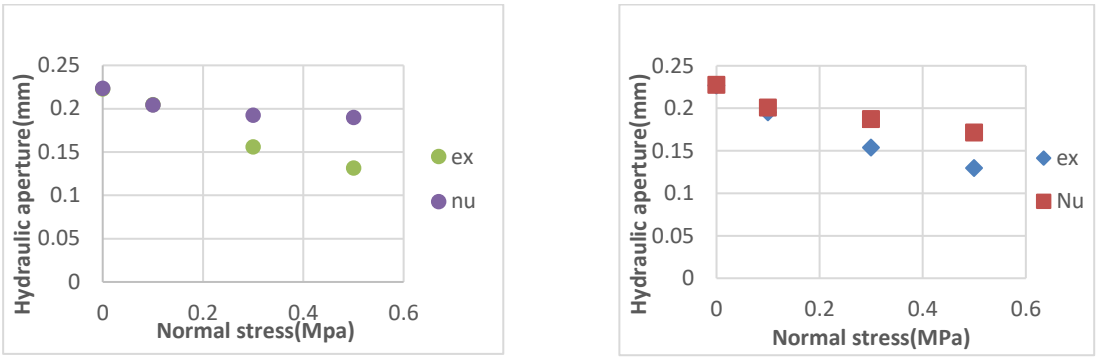

(a) (b)

Figure 8. Hydraulic apertures obtained from experimental and numerical modeling, (a) through direction X and (b) direction Y.

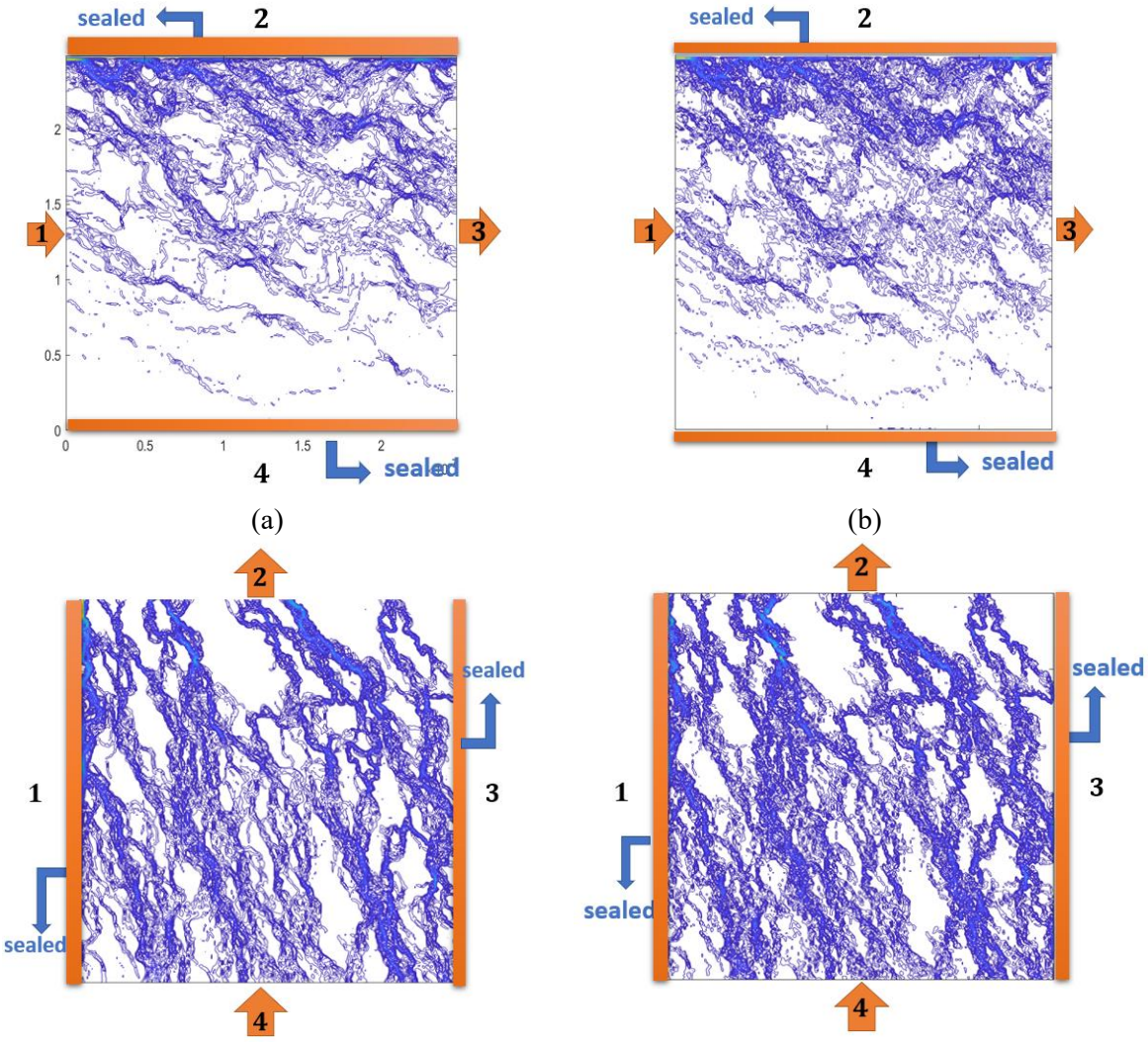

(a) (b)

(c) (d)

Figure 9. Simulation of streamlines inside the fracture in two different directions, (a) water pressure 5 kPa and (b) 50 kPa with normal stress 0 MPa, (c) water pressure 5 kPa and (d) 50 kPa with normal stress 0.5 MPa.

4. Conclusions

In this research, 80 water flow tests were conducted through a 250 mm × 250 mm fracture in two perpendicular directions under applying four normal stresses 0, 0.1, 0.3 and 0.5 MPa with ten water pressures ranging from 5 kPa to 50 kPa with a 5 kPa interval. The experimental data (relationship between flow rate and pressure gradient) were expressed by the Forchheimer equation. Photogrammetric method was used to reconstruct the fracture surface and determine its physical aperture. Numerical modeling was performed to analyze the flow behavior inside the fracture. The reconstructed fracture was rasterized with a 1 mm grid interval. The hydraulic apertures for different directions and in the abovementioned conditions were calculated based on the Forchheimer equation for the experimental and numerical modeling. The differences between experimental hydraulic apertures in perpendicular directions are almost 7%, and numerical hydraulic apertures are near 4%. It means the fracture surface is anisotropic, although it seems homogenous with a visual inspection. Also, numerical modeling shows different patterns of flow streamlines through perpendicular directions. The numerical modeling versus experimental water flow tests shows a good match at 0 and 0.1 MPa and almost 50 % deviation at higher pressures 0.3 MPa and 0.5 MPa.

Acknowledgments

The authors gratefully thank the Finnish Nuclear Waste Management fund VYR and the KYT2022 research programme for funding.

References

[1] Koyama T, Fardin N, Jing L and Stephansson O 2006 Numerical simulation of shear-induced flow anisotropy and scale-dependent aperture and transmissivity evolution of rock fracture replicas *Int. J. Rock Mech. Min.* **43**(1) 89-106.
[2] Sun J and Zhao Z 2010 Effects of anisotropic permeability of fractured rock masses on underground oil storage caverns *Tunn. Undergr. Space Technol.* **25**(5) 629-637.
[3] Zhang Y and Chai J 2020 Effect of surface morphology on fluid flow in rough fractures: a review *J. Nat. Gas Sci. Eng.* **79** 103343.
[4] An P, Fang K, Jiang Q, Zhang H and Zhang Y 2021 Measurement of rock joint surfaces by using smartphone structure from motion (SfM) photogrammetry *Sens.* **21**(3) 922.
[5] Yang H, Wang X, Yu L and Liu R 2021 Effects of contact area and contact shape on nonlinear fluid flow properties of fractures by solving Navier-Stokes equations *Lithosphere* **2021**(Special 3) 8684428.
[6] Auradou H, Hulin JP and Roux S 2001 Experimental study of miscible displacement fronts in rough self-affine fractures *Phys. Rev. E* **63**(6) 066306.
[7] Gentier S, Lamontagne E, Archambault G and Riss J 1997 Anisotropy of flow in a fracture undergoing shear and its relationship to the direction of shearing and injection pressure *Int. J. Rock Mech. Min.* **34**(3-4) 94-e1.
[8] Méheust Y and Schmittbuhl J 2001 Geometrical heterogeneities and permeability anisotropy of rough fractures *J. Geophys. Res. Solid Earth* **106**(B2) 2089-2102.
[9] Marchand S, Mersch O, Selzer M, Nitschke F, Schoenball M, Schmittbuhl J, Nestler B and Kohl T 2020 A stochastic study of flow anisotropy and channelling in open rough fractures *Rock Mech. Rock Eng.* **53**(1) 233-249.
[10] Deng Q, Blöcher G, Cacace M and Schmittbuhl J 2021 Hydraulic diffusivity of a partially open rough fracture *Rock Mech. Rock Eng.* **54**(10) 5493-5515.
[11] Qian X, Xia C, Gui Y, Zhuang X and Yu Q 2019 Study on flow regimes and seepage models through open rough-walled rock joints under high hydraulic gradient *Hydrogeol. J.* **27**(4) 1329-1343.